INTERNATIONAL JOURNAL OF AUTOMOTIVE AND MECHANICAL ENGINEERING
ISSN: 2229-8649 e-ISSN: 2180-1606
VOLUME 22, ISSUE 4, 2025, 12933 - 12942
DOI: https://doi.org/10.15282/ijame.22.4.2025.7.0984

RESEARCH ARTICLE

Impact of Throat Diameter, Length, and Divergent Angle on Bubble Formation and Flow Characteristics in Venturi Microbubble Generators

N. Nadumaran[1], EA.Alias[1,2]*

[1]Faculty of Manufacturing and Mechatronic Engineering Technology, Universiti Malaysia Pahang Al-Sultan Abdullah, 26600 Pahang, Malaysia
[2]Centre for Research in Advanced Fluid and Processes, Universiti Malaysia Pahang Al-Sultan Abdullah, 26600 Pahang, Malaysia

ABSTRACT – The design of a Venturi microbubble generator (VMBG) is crucial in influencing the size and distribution of produced microbubbles, which are essential in several industrial, medicinal, and environmental applications. This study examines the impact of three critical geometric parameters: throat diameter, throat length, and divergent angle, on the formation of bubbles and the characteristics of flow. A combination of experimental visualization using Particle Image Velocimetry and computational fluid dynamics simulations using the Euler–Lagrange approach with the realizable k-epsilon turbulence model was employed. Nine VMBG configurations were tested, with throat diameters of 8.5 mm, 12 mm, and 20 mm, throat lengths of 10 mm, 15 mm, and 30 mm, and divergent angles of 30°, 45°, and 60°. The findings showed that decreasing the throat diameter from 12 mm to 8.5 mm produced smaller and denser bubbles, resulting in an increase in flow velocity by 68% and vorticity by 30%. Results showed that smaller throat diameters (8.5 mm) increased flow velocities, turbulence, and vorticity, while longer throat lengths (30 mm) provided smoother fluid transitions. Larger divergent angles caused a significant drop in velocity, increased turbulence, and produced smaller bubble sizes. However, they also promoted bubble expansion and denser formation in the divergent section. Both throat diameter and throat length also played a crucial role in undergoing complete bubble formation stages. Experimental results, which were very similar to the computer results, verified the four stages of bubble formation: nucleation, expansion, coalescence, and breakdown. The study provides valuable insights for enhancing VMBG designs, enabling the creation of microbubbles with features suitable for specific applications.

ARTICLE HISTORY
Received : 27th Sept. 2024
Revised : 20th June 2025
Accepted : 22nd Aug. 2025
Published : 18th Nov. 2025

KEYWORDS
Bubble formation
Throat diameter
Throat length
Divergent angle
Venturi
Microbubble

1. INTRODUCTION

The venturi microbubble generator (VMBG) operates by creating low-pressure zones that promote fluid movement and enhance cavitation, thereby facilitating the generation of microbubbles (MB) [1], [2]. The application of this technology spans various sectors, including agriculture [3], aquaculture [4], [5], medical treatment [6], [7], flotation [8], the automotive industry [9], [10], oil recovery [11], and marine engineering [12]. Controlling the generated size distribution of MB is essential for optimizing performance in these applications, as each application requires a specific size distribution.

The size and distribution of MB are notably affected by the flow characteristics present within the geometry, which are contingent upon the geometrical configuration of the venturi and the prevailing flow conditions [1], [12], [13]. Previous studies have focused on how changes in throat diameter, throat length, and divergent angle affect bubble size and distribution in geometric configurations. The diameter of the throat influences the fluid velocity within the VMBG, where reduced diameters result in increased velocities and a greater potential for cavitation [14]. The study conducted by Huang et al. [15] revealed that a decrease in throat diameter notably enhances turbulence intensity and hastens the formation of MB, thereby improving the efficiency of processes such as oxidation and mixing. Furthermore, investigations conducted by Safreena et al. [16] revealed that reduced throat diameters result in a more significant pressure drop, thereby increasing the nucleation rate and regulating the size distribution of the produced bubbles. Optimizing the throat diameter is essential for customizing bubble characteristics and enhancing the performance of Venturi-based systems across various industrial applications.

Throat length, on the other hand, impacts the residence time of the fluid within the low-pressure zone, thereby influencing the extent of cavitation and microbubble formation [14], [15]. Research by Ullas et al.[17] highlighted that longer throat lengths increase the fluid's exposure time to low-pressure conditions, enhancing bubble growth and stability by allowing more nucleation and coalescence processes. Similarly, Sidhi et al. [18] found that optimizing throat length can reduce turbulence and improve bubble size consistency, making it crucial for applications requiring precise bubble control and efficient mass transfer. These findings underscore the importance of carefully designing throat length to balance fluid dynamics and maximize microbubble generation efficiency in Venturi-based systems.

***CORRESPONDING AUTHOR | E. A. Alias** | ✉ erny@umpsa.edu.my

The divergence angle is crucial in determining the fluidity of a constriction and its interaction with the environment, thereby affecting the generation and size distribution of bubbles. Prior studies have examined the impact of the divergent angle on flow reattachment and turbulence [9], [10], [11]. Subsequent research indicates that a larger divergent angle can promote smoother flow expansion and mitigate flow separation, thereby improving bubble stability and distribution [19], [20]. Nadumaran et al. [2] also found that optimizing the divergent angle enhances microbubble generation by reducing vortex formation and ensuring that the bubbles are all the same size. This demonstrates the importance of having precise control over bubble characteristics in VMBG systems [21]. Table 1 presents a structured comparison of earlier works to highlight the focus, methods, and limitations of the selected studies on VMBG geometry.

Table 1. The summary of past studies on VMBG geometric parameters

Study	Parameter Investigated	Method Used	Key Findings	Limitations
Huang et al. [15]	Throat diameter	Experimental	Smaller diameters increase turbulence and cavitation	No CFD validation
Safreena et al. [16]	Throat diameter	Simulation	Pressure drop enhances bubble nucleation	Only a single parameter studied
Ullas et al. [17]	Throat length	Experimental	Longer throats increase residence time	No link to bubble size
Sidhi et al. [18]	Throat length	Experimental + CFD	Flow stability improves with optimized length	Divergent angle not considered
Zhao et al. [19]	Divergent angle	Experimental	Larger angles increase recirculation and breakup	Throat geometry not analyzed
Nadumaran et al. [2]	Divergent angle	CFD	Bubble breakup is sensitive to angle	Lacks experimental support

While earlier investigations have explored the separate influences of throat diameter and throat length on bubble formation in VMBGs, a comprehensive understanding of their combined effects remains lacking. The impact of throat diameter on fluid velocity and bubble nucleation is well-established [16]. However, the comparative influence of throat diameter and throat length on overall bubble production efficiency remains to be thoroughly investigated [1], [22]. Furthermore, the divergent angle has also been shown to influence bubble dynamics and flow patterns [23]. However, its role in optimizing bubble formation in conjunction with throat diameter and length has not been thoroughly explored. Most existing studies focus on isolated parameter effects and rely predominantly on either experimental or computational analysis [15], [20], leading to limited cross-validation and incomplete flow characterization. Therefore, there is a critical need for an integrated approach that combines experimental visualization and computational fluid dynamics (CFD), which holistically assesses how these geometric parameters collectively influence flow behavior and bubble formation in VMBGs. Moreover, the lack of integration between CFD simulations and experimental validation further restricts the generalizability of past findings.

To address these gaps, the present study investigates the combined effects of throat diameter, throat length, and divergent angle on bubble formation characteristics in VMBGs. A dual technique comprising experimental testing with Particle Image Velocimetry (PIV) and numerical simulation utilizing the Euler-Lagrange model with the realizable k-epsilon turbulence model was employed. The objective of this study is to (i) examine the flow characteristics and bubble formation stages across different geometries, (ii) validate CFD results against experimental observations, and (iii) identify optimal design parameters to improve microbubble generation performance. The insights gained will be useful for managing the distribution of generated MB sizes and enhancing performance for a variety of applications.

2. METHODS AND MATERIAL

2.1 Experimental Visualization

The experimental visualization setup is illustrated in Figure 1, comprising a venturi, a water tank, a pump, and a PIV system. A total of six venturis with different throat diameters, lengths, and divergent angles were designed using SolidWorks 2020, a 3D design software. The detailed dimensions and design for all venturis are provided in Table 2 and Figure 2(a) and 2(b), respectively. Figure 3 shows the actual view of the experimental setup.

The VMBGs were fabricated through CNC machining using acrylic material to maintain transparency for visualization purposes. In the experiment, water was used as the working fluid, and the VMBG was secured in a test rig measuring 800 mm × 600 mm × 519 mm. A pump with 0.75 hp and 550 W was utilized to provide pressurized water to the VMBG, while another pump was used to circulate the water from the observation tank to the supply tank. The water flow rate was controlled using a ball valve and kept constant at 70 LPM. The PIV setup was used to observe the flow pattern and bubble formation between the throat and divergent sections of the VMBG. For calibration, it was performed on a defined plane to ensure laser alignment and accuracy. The camera and laser were fixed in place after calibration to maintain consistency

throughout data capture. The transverse stage was used to reposition the laser sheet and camera during scanning. Captured images were processed in Dynamic Studio software to extract velocity vectors and track tracer particles.

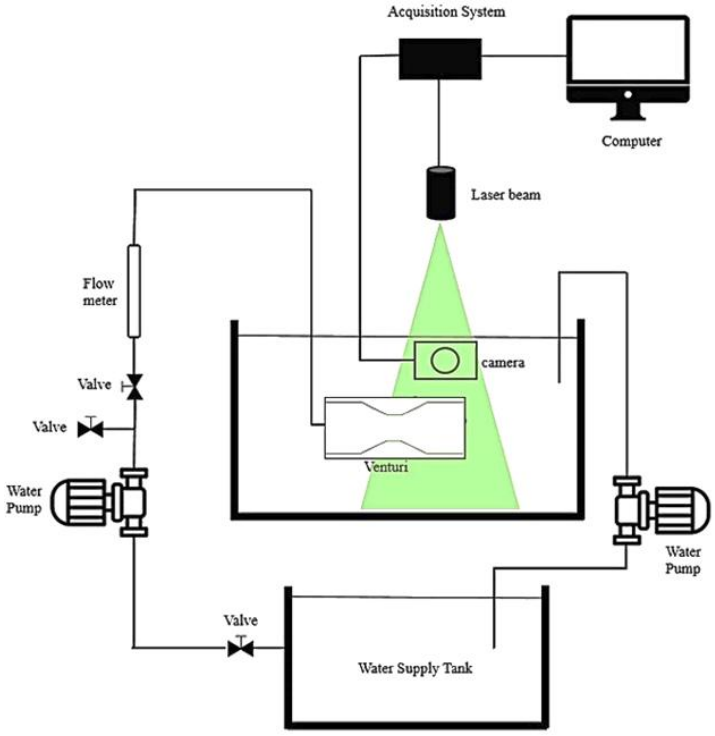

Figure 1. Experiment setup used

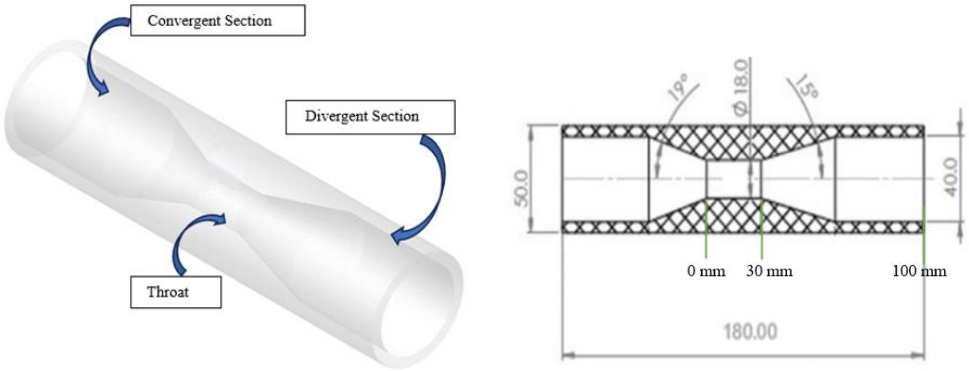

(a) (b)

Figure 2. (a) The 3D drawing of the ideal venturi, (b) The dimensions of the ideal venturi

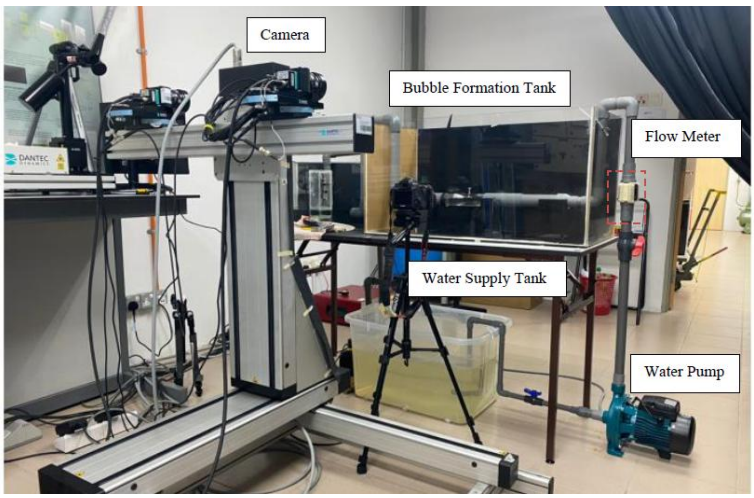

Figure 3. Actual view of the experimental setup

Table 2. The dimension of the fabricated VMBG

VMBG	Convergent Angle	Divergent Angle	Throat Diameter (mm)	Throat Length (mm)
V1	19°	15°	8.50	20
V2	19°	15°	12.50	20
V3	19°	15°	20.00	20
V4	19°	15°	11.11	10
V5	19°	15°	11.11	15
V6	19°	15°	11.11	30
V7	19°	30°	11.11	20
V8	19°	45°	11.11	20
V9	19°	60°	11.11	20

2.2 Computational Analysis

A similar design of VMBG was utilized in a computational simulation analysis to obtain detailed flow characteristics. The virtual model was developed, with CFD selected as the Physics Preference and Fluent as the Solver Preference. A mesh independence test was conducted for the VMBG (V1) to ensure that the mesh size did not influence the results. The mesh quality, including orthogonal quality, skewness, and aspect ratio, was evaluated to determine the most suitable type of mesh for use throughout the study. The element size varied from 0.4 mm to 0.7 mm for the VMBG. A mesh independence study was conducted on VMBG 1 using element sizes from 0.7 mm to 0.4 mm. Results showed a difference of less than 1% in average velocity between the 0.5 mm and 0.4 mm meshes, confirming that 0.5 mm was sufficiently accurate and could be used for all models, as shown in Figure 4.

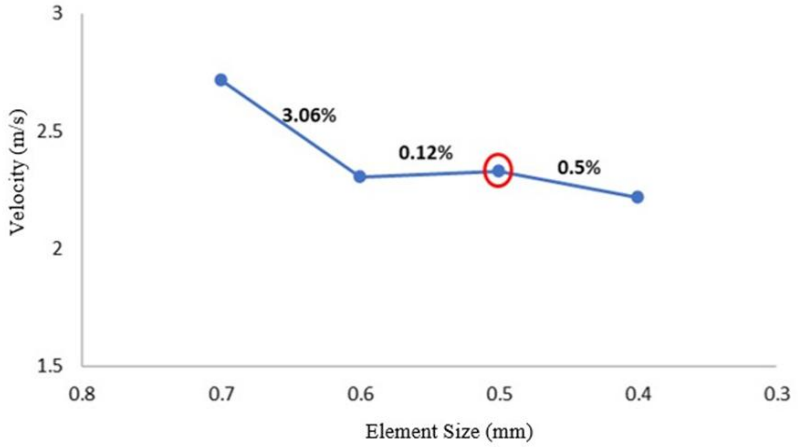

Figure 4. Velocity graph of mesh independence study

For the solver setup, the Euler-Lagrange flow model was employed to analyze the flow of the VMBG [22], [24]. Additionally, the realizable k-ε turbulence model was utilized to account for the effects of turbulence. The simulation employed the Euler–Lagrange multiphase approach to model water and air interaction, with turbulence effects captured using the realizable k–ε model due to its improved accuracy in swirling and separated flows, particularly in diffuser-type geometries[21], [25], [26]. The pressure at the outlet was maintained at 1 atm, while the inlet velocity was set according to a 70 L/min flow rate. The inlet velocity was calculated using the continuity equation. As for the wall condition, a non-slip boundary condition was implemented. The control equations were discretized using the finite volume method, and the velocity-pressure coupling was solved by employing the semi-implicit pressure-linked equation (SIMPLE) method. The primary physical properties of the model setup are provided in Table 3.

Table 3. The physical properties of water

Fluid Property	Value and Unit
Liquid (water) density	998.2 kg/m^3
Liquid (water) dynamic viscosity	0.001003 kg/m·s
Gravity acceleration	9.81 m/s^2

Convergence was achieved when residuals dropped below 1×10^{-4} for all continuity and momentum equations. Temporal stability and convergence of transient solutions were monitored using velocity probes at key locations.

3. RESULTS AND DISCUSSION

3.1 Effect of Different Geometry Parameters on Flow Characteristics

3.1.1 Effect of throat diameter on flow characteristics

Figure 5(a) illustrates the velocity distribution along the throat and divergent sections in all VMBGs. The relationship between throat diameter and fluid velocity shows that the velocity increases as the cross-sectional area (throat diameter) decreases [16], [17], [22], [27]. The same phenomenon can be seen in venturis with different throat diameters (V1, V2, and V3). In the case of V1, a significant drop in velocity of 1.5123 m/s after the throat, as the fluid exits into the divergent section, is found due to the sudden expansion of the divergent section after the throat section. For V2 and V3, larger throat diameters result in stable flow with less velocity variation [16], [22]. The closer throat and outlet diameters allow for smoother fluid transition, maintaining nearly constant velocity at the exit [28].

Table 4 illustrates the flow characteristics, including experimental visualization images, velocity vectors, and vorticity contours, within the VMBGs. In general, experimental findings indicate that bubble formation only occurs in the VMBG with the smallest throat (V1) and not in the other throat diameters. Recirculation flow occurs in all VMBGs at the divergent section, with the high-velocity region occurring on the upper side in V1 and the lower side in V2 and V3. Recirculation zones appear much earlier for V1 than V2 and V3, indicating high vorticity and denser bubble formation in the VMBG (Table 3) [14], [29]. Overall, the venturi with the smallest throat diameter (in this study, 8.5 mm) produced a smaller and greater density of bubbles due to a 30% increase in vorticity, as calculated by comparing the average vorticity magnitude in the divergent section for V1 against V3 using CFD post-processing tools in ANSYS Fluent. The data is further supported by the findings from [14], [30], which showed that the smallest bubble is produced from VMBG with a smaller throat diameter.

3.1.2 Effect of throat length on flow characteristics

As shown in Figure 5(b) (velocity distribution), the venturi with the longest throat (V6) illustrates the highest velocity rise compared to other VMBGs at the throat section. On the other hand, V4 exhibits a quicker transition in bubble formation compared to V5 and V6. Thus, the findings conclude that as the length of the throat increases, the velocity rise in the throat also increases and accelerates more rapidly. Conversely, a shorter throat would cause the fluid to accelerate more rapidly [31].

As for the flow characteristics for venturis with different throat lengths, as shown in Table 4, experimental findings indicate that bubble formation occurs in the VMBG with the shorter throat length (V4 and V5) and not in V6, which has the longest throat length. It is observed that the maximum velocities of 3.466 m/s, 3.095 m/s, and 2.59 m/s at the throat section for V4, V5, and V6, respectively, indicate the effect of throat length on flow velocity along the throat area. This shows that the velocity in a longer throat (V6) results in gradual velocity recovery compared to V4 and V5. In addition, the length of the throat also impacts the vorticity distribution, which leads to the disintegration of gases in the VMBG, with Table 4 illustrating that V4 and V5 exhibit slightly lower vorticity from the throat section to the divergent section compared to V6. Findings show that the length of the throat can influence the strength and formation of these vortices, affecting the vorticity levels in the flow field and thereby impacting the dispersion and interaction of bubbles within the flow.

3.1.3 Effect of divergent angle on flow characteristics

As for the comparison between different divergent angles (VMBG 7, 8, and 9) in Figure 5(c), the venturi with the larger divergent angles (V9) shows a great drop in velocity after the throat section. The results indicate a greater velocity drop after the throat section as the divergent angle increases. VMBGs with 30º and 45º divergent angles (V7 and V8) show a similar trend, with average velocities of 4.849 m/s and 4.337 m/s, respectively, while V9 has an average velocity of 3.114 m/s. The velocities in V7 and V8 are higher, but the divergent angle is too large, leading to rapid velocity recovery at the divergent section. These findings are consistent with those of a previous study [20], [23], [31], [32].

Regarding the effect of divergent angles on flow characteristics, as shown in Table 3, experimental findings indicate that bubble formation occurs in all VMBGs. Table 4 also shows the velocity vector plots illustrating the presence of a recirculation zone at the wall in all VMBGs, with the largest occurring in the venturi with the largest divergent angle (V9). The presence of recirculation zones in the divergent section generates higher vorticity levels. This initiates longer bubble residence times within the divergent section [32], [33]. Bubbles tend to be trapped or recirculated within these zones for a longer duration, which can result in smaller bubbles [33]. The findings also show irregular vorticity at V8 and V9. This is because sudden expansion in the divergent section triggers the onset of vorticity [19], [32], [33].

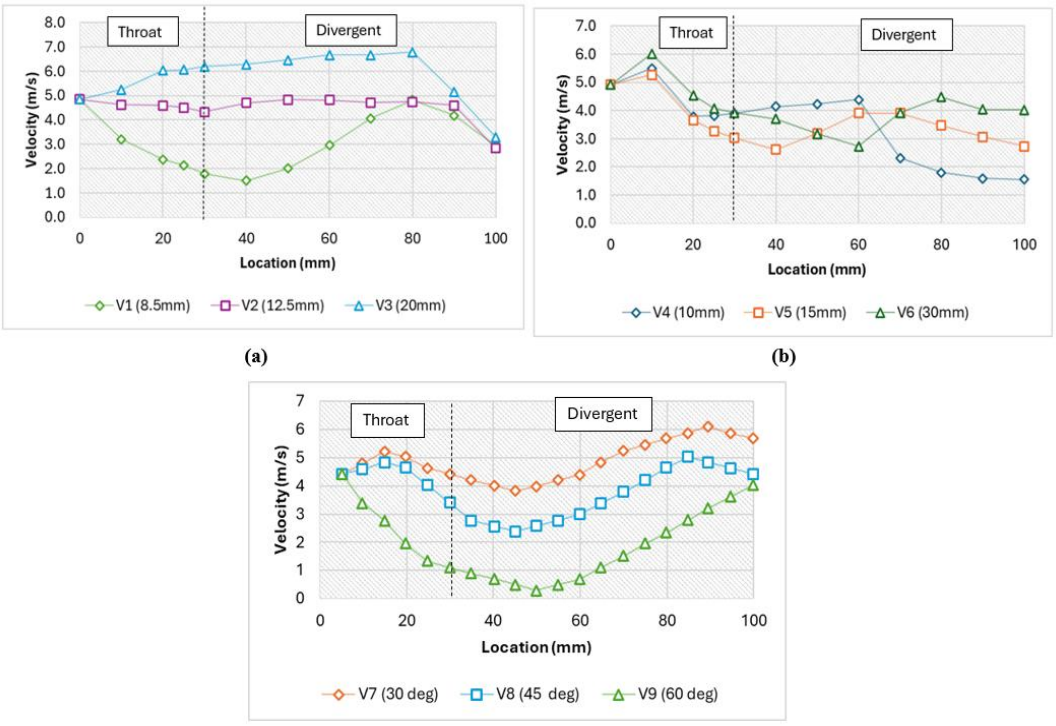

Figure 5. (a) The velocity distribution of different throat diameters, (b) velocity distribution of different throat lengths and (c) velocity distribution of different divergent angles

Table 4. The outcome of bubble formation (experimental result), flow vectors (computational result), turbulent intensity (computational result) and vorticity (computational result) of different geometry parameters

Parameters	Bubble formation	Flow vector	Turbulent intensity	Vorticity
Throat diameter	V1			
	V2			
	V3			
Throat length	V4			
	V5			
	V6			
Divergent angle	V7			
	V8			
	V9			

3.2 Bubble Formation Characteristics in VMBGs

3.2.1 Bubble formation characteristics in VMBG with different throat diameters

Table 4 illustrates the detailed bubble formation in V1 at a flow rate of 70 LPM. The bubble formation data is organized as follows: V1 is shown in the first row, V4 in the second row, and V9 in the third row. Overall, V1 experiences the four stages of the bubble nucleation (cavitation) formation phenomenon: bubble nucleation, bubble growth, bubble coalescence, and bubble breakup. At 0.0 ms (milliseconds), the bubble starts to form at the upper corner of the throat. The elongation of bubbles continues at 1.2 ms until 2.4 ms. The bubble starts to break up at 3.6 ms. Between 4.8 ms and 6.0 ms, the bubble breaks up more significantly, resulting in the generation of finer and more dispersed bubbles. This occurred due to the turbulent intensity and vorticity, which enhanced the bubble breakup [15], [34]. Thus, the diameter of the throat can be considered one of the prominent geometric parameters that can be controlled to obtain the desired microbubble sizes [35]. In summary, experimental findings on formation phenomena, supported by simulation results, demonstrate that a small throat diameter increases flow velocities, associated vorticity, and turbulent intensity [34]. This may result in slow bubble breakup and dispersion, leading to the formation of smaller and denser bubbles. Thus, the throat diameter can be considered one of the prominent geometric parameters that can be controlled to obtain the desired microbubble sizes [15], [35].

3.2.2 Bubble formation characteristics in VMBG with different throat lengths

Table 5 illustrates the bubble formation characteristics in V4 at 70 LPM. At 0.0 ms, V4 experiences bubble cavitation at the upper corner end of the throat. In 2.4 ms, the bubble starts to break up in V4. It experiences continuous bubble breakup from 3.6 ms to 6.0 ms. From the results, changes in throat length may impact the flow dynamics and the ability to maintain a stable flow regime. Findings prove that the length of the throat can affect the dispersion and interaction of bubbles within the flow [30]. These variations in velocity and turbulence, coupled with vorticity, influence the formation of bubbles. The data is further supported by the findings from [17], [31], which obtained the same findings on bubble formation by using different throat lengths.

3.2.3 Bubble formation characteristics in VMBG with different divergent angles

Table 5 presents the experimental visualization of the detailed bubble formation characteristics in V9, along with the turbulent intensity contours obtained from computational simulation at 70 LPM. In general, all three VMBGs experience the four stages of the formation phenomenon of bubble nucleation (cavitation), bubble growth, bubble coalescence, and bubble breakup. V9 shows the bubble cavitation at 0.0ms, then elongates at 1.2 ms. At 2.4 ms, the bubble continues to elongate. The bubble in V9 begins to break up at 3.6 ms. At 6.0 ms, the experimental findings illustrate that V9 produces a much denser number of bubbles compared to V4. A larger divergent angle can promote faster bubble expansion and stretching due to decreased flow velocities [23]. This phenomenon also indicates denser bubble formation in the divergent section. Besides, rapid expansion can also cause bubbles to reach their maximum size more quickly, resulting in smaller bubbles being formed overall (as shown in the red circle in Table 5 at 2.4 ms).

Table 5. The outcome of bubble formation (experimental result) in all VMBGs

Parameters	Bubble formation images in 6ms
Throat Diameter	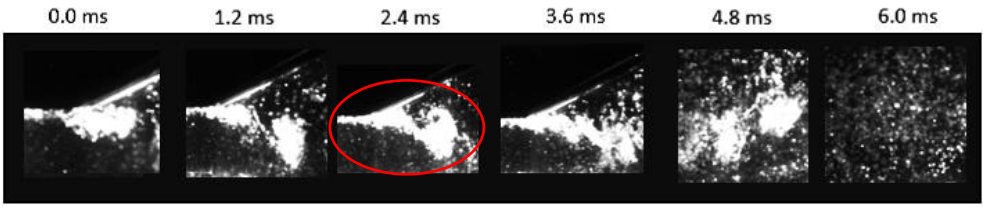
Throat length	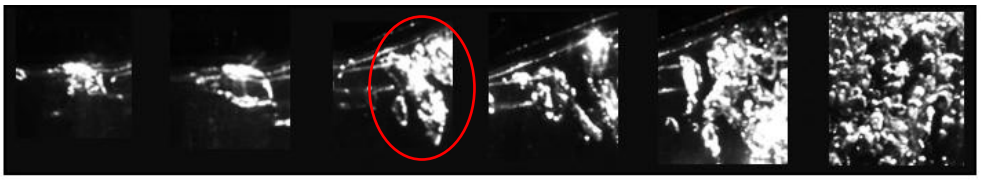
Divergent angle	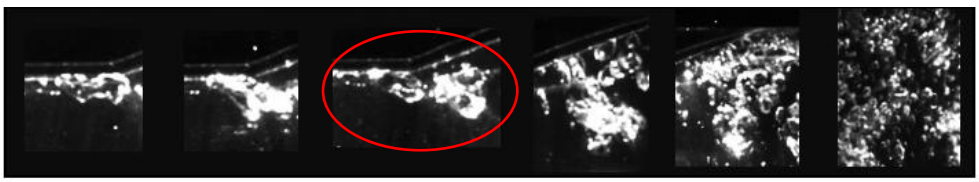

This finding is supported by several works regarding the bubble collapse or breakup in a VMBG [29], [30], [31], [36]. In summary, experimental findings on the bubble formation phenomenon, supported by the flow characteristics, show that a larger divergent angle leads to a more intensive bubble breakup process, resulting in a higher density of smaller bubbles compared to a smaller divergent angle [37].

Overall, the bubble formation with different geometry parameters is further supported by the simulation findings, namely, velocity distribution, turbulent intensity, vorticity, and velocity vector. Due to these changes in velocity distribution, turbulent intensity, and vorticity, a bubble experiences four main stages of formation characteristics, which are bubble nucleation (cavitation), bubble growth, bubble coalescence, and bubble breakup, as summarized in Table 6.

Table 6. The summarized outcome of computational simulation and experimental visualization

Parameter	Throat Diameter	Throat Length	Divergent Angle
Impact on Velocity	Higher flow velocities	More gradual increase in velocity	Affects deceleration and recirculation of flow
Impact on Vorticity	More pronounced vorticity	Affects the strength of vortices	Promotes vorticity at divergent walls
Impact on Turbulence	Greater turbulent intensity	Affects bubble interaction	Influences the spread and turbulence near walls
Bubble Characteristics	Smaller and denser bubbles	Larger, elongated bubbles with reduced turbulence	Finer bubbles with greater breakup potential

4. CONCLUSIONS

This study investigated the impact of three important geometric factors, such as throat diameter, throat length, and diverging angles, on bubble generation and flow in VMBGs. These factors are significant for bubble formation in both experimental imaging with Particle Image Velocimetry (PIV) and computational fluid dynamics (CFD) simulations. Comparison in terms of throat diameter shows that the reduction of diameter from 12.5 mm to 8.5 mm increased the flow velocity by 68%, apparently, this also increases turbulence and vorticity. Thus, the bubbles generated were smaller and denser. This result was the same in both experimental and simulation data. Besides, longer throat length reduces the turbulence and makes the flow more stable, while shorter throat lengths accelerate the flow and induce stronger vorticity. This resulted in a longer throat producing bigger and more stable bubbles, while a shorter throat produced smaller and denser bubble formation. Lastly, the diverging angle had a significant impact on velocity and turbulence in the VMBG. Angles of up to 60° caused the velocity to drop greatly after the throat. This made it easier for bubbles to grow and circulate more, which led to smaller bubbles. Bubbles stayed in the water longer than in a larger divergent angle.

The study demonstrates that the throat diameter, throat length, and diverging angle play vital roles in the generation of microbubbles. The results showed how different geometric parameters affected the bubbles' size, speed, turbulence, and vorticity. This showed how geometry affects bubble properties. To get the desired bubble characteristics for applications in areas such as water treatment, biomedical devices, and environmental systems, it is essential to meticulously adjust these parameters. The study also revealed that CFD simulations were accurate by comparing them to experimental data from PIV. The validation confirmed that the CFD model could properly predict microbubble production and flow dynamics. Researchers need to examine how flow rates and increasingly complex fluid behaviors impact VMBG designs for various applications in the future.

ACKNOWLEDGEMENTS

The authors are grateful to the Ministry of Higher Education Malaysia and Universiti Malaysia Pahang (www.ump.edu.my) for financial support given under FRGS/1/2022/TK08/UMP/02/26 (RDU220115), RDU220339 and PGRS220327. The authors would also like to express gratitude to the Centre for Research in Advanced Fluid, Universiti Malaysia Pahang Al-Sultan Abdullah, for insight and expertise that greatly assisted the present research work.

CONFLICT OF INTEREST

The authors declare no conflicts of interest.

AUTHORS CONTRIBUTION

N. Nadumaran (Formal analysis; Visualization; Data curation; Writing – Original Draft)

E.A. Alias (Conceptualization; Validation, Writing – review & editing; Funding acquisition; Resources; Supervision)

REFERENCES

[1] K. Sakamatapan, M. Mesgarpour, O. Mahian, H. S. Ahn, S. Wongwises, “Experimental investigation of the microbubble generation using a venturi-type bubble generator,” *Case Studies in Thermal Engineering*, vol. 27, pp. 101238, 2021.

[2] N. Nadumaran, E. A. Alias, M. H. Hamidi, N. H. Johari, "Effect of divergent angle and water flowrate on mean bubble size in venturi-type generator: An experimental and computational approach," *Journal of Mechanical Engineering and Sciences*, vol. 19, no. 2, pp. 10667-10675, 2025.

[3] Y. He, T. Zhang, L. Lv, W. Tang, Y. Wang, J. Zhou, et al., "Application of microbubbles in chemistry, wastewater treatment, medicine, cosmetics, and agriculture: a review," *Environmental Chemistry Letters*, vol. 21, no. 6, pp. 3245-3271, 2023.

[4] I. Taukhid, A. Dirpan, Misbah, M. I. Mukhsen, Ariyanto, B. R. Tampangallo, "Microbubble generator to support aeration for aquaculture: A bibliometric analysis," *Thalassas: An International Journal of Marine Sciences*, vol. 41, no. 3, p. 130, 2025.

[5] R. Fitriadi, M. Palupi, "Application of microbubble technology to increase oxygen content in the aquaculture of tambaqui (Colossoma macropomum)," *Journal of Aquaculture and Fish Health*, vol. 13, no. 3, pp. 328-339, 2024.

[6] V. S. Ganesh, K. V. Venkatesh, D. Sihivahanan, P. K. Yadalam, D. Shrivastava, K.C. Srivastava, "Effect of microbubble as local drug delivery system in endodontic management – An in-vitro study," *Saudi Dental Journal*, vol. 36, no. 6, pp. 863-867, 2024.

[7] T. Saliev, M. Akishev, "Ultrasound binary microbubble drug delivery and drug synthesis for cancer treatment," *Journal of Analytical Science & Technology*, vol. 16, no. 1, p. 11, 2025.

[8] Z. Chang, S. Niu, Z. Shen, L. Zou, H. Wang, "Latest advances and progress in the microbubble flotation of fine minerals: Microbubble preparation, equipment, and applications," *International Journal of Minerals, Metallurgy and Materials*, vol. 30, no. 7, pp. 1244-1260, 2023.

[9] E.A. Alias, H. Okanaga, "Effect of skin friction reduction by microbubbles in pipe flow," *Proceedings of the School of Engineering of Tokai University*, vol. 37, pp. 23-27, 2021.

[10] A. Erny, D. Fatimah, I. Muhammad, "Fundamental characteristics of microbubbles in water and diesel fuel," in *MATEC Web of Conferences*, EDP Sciences, vol. 225, p. 05015, 2018.

[11] N.A. Mohd Pouzi, E.A. Alias, M. Pira, D. Mani, S.H. Norazman, "An experimental study on the efficiency of microbubbles in enhance oil recovery method (EOR) in different types of oils," *Journal of Advanced Research in Experimental Fluid Mechanics and Heat Transfer*, vol. 20, no. 1, pp. 30-40, 2025.

[12] A. García-Magariño, S. Sor, R. Bardera, P. López-Gavilán, "Theoretical model for microbubble drag reduction technique applied to marine propellers," *Ocean Engineering*, vol. 329, pp. 120797, 2025.

[13] Y. Song, R. Xu, K. Cai, J. Yin, D. Wang, "Numerical studies on bubble dynamics in an unsteady turbulence of the venturi bubble generator applied to TMSR," *Annals of Nuclear Energy*, vol. 160, p. 108322, 2021.

[14] D.A. Wilson, K. Pun, P.B. Ganesan, F. Hamad, "Geometrical optimization of a venturi-type microbubble generator using CFD simulation and experimental measurements," *Designs*, vol. 5, no. 1, p. 4, 2021.

[15] J. Huang, L. Sun, Z. Mo, Y. Feng, J. Bao, J. Tang, "Experimental investigation on the effect of throat size on bubble transportation and breakup in small Venturi channels," *International Journal of Multiphase Flow*, vol. 142, p. 103737, 2021.

[16] N. Saffreena, A. Kaneko, "Effect of throat size on pressure and void fraction fluctuation in venturi tube microbubble generator," in *Lecture Notes in Mechanical Engineering*, Springer, pp. 325-329, 2024.

[17] P.K. Ullas, D. Chatterjee, S. Vengadesan, "Experimental study on the effect of throat length in the dynamics of internal unsteady cavitating flow," *Physics of Fluids*, vol. 35, no. 2, p. 023332, 2023.

[18] S.D.P. Sidhi, A. Pujianto, A. Nurfauzi, D. Prasetyo, B. Basino, M.A. Ansori, et al., "Improving the performance of microbubble through the modification and optimization of venturi-type generator," *Jurnal Polimesin*, vol. 22, no. 2, p. 211, 2024.

[19] L. Zhao, L. Sun, Z. Mo, J. Tang, L. Hu, J. Bao, "An investigation on bubble motion in liquid flowing through a rectangular venturi channel," *Experimental Thermal and Fluid Science*, vol. 97, pp. 48-58, 2018.

[20] L. Zhao, L. Sun, Z. Mo, M. Du, J. Huang, J. Bao, et al., "Effects of the divergent angle on bubble transportation in a rectangular venturi channel and its performance in producing fine bubbles," *International Journal of Multiphase Flow*, vol. 114, pp. 192-206, 2019.

[21] W. Wang, X. Zhang, C. Li, Y. Zou, G. Li, Y. Chen, et al., "Bubble behavior, flow characteristics, and mass transfer enhancement in self-priming Venturi tubes," *Chemical Engineering Science*, vol. 270, p. 118536, 2023.

[22] X. Vilaida, S. Kythavone, T. Iijima, "Effect of throat size on performance of microbubble generator and waste water treatment," in *IOP Conference Series: Materials Science and Engineering*, vol. 639, no. 1, p. 012031, 2019.

[23] J. Chen, M. Lei, S. Lu, X. Xiao, M. Yao, Q. Li, "Numerical simulation of single bubble motion fragmentation mechanism in venturi-type bubble generator," *Mechanics and Industry*, vol. 25, p. 21, 2024.

[24] Y. Song, Y. Shentu, Y. Qian, J. Yin, D. Wang, "Experiment and modeling of liquid-phase flow in a venturi tube using stereoscopic PIV," *Nuclear Engineering and Technology*, vol. 53, no. 1, pp. 79–92, 2021.

[25] L. Zhang, L. Tian, Q. Shen, F. Liu, H. Li, Z. Dong, et al., "Study on the influence and optimization of the venturi effect on the natural ventilation of buildings in the Xichang area," *Energies*, vol. 14, no. 16, p. 5053, 2021.

[26] P. Pipp, M. Hočevar, M. Dular, "Challenges of numerical simulations of cavitation reactors for water treatment – An example of flow simulation inside a cavitating microchannel," *Ultrasonics Sonochemistry*, vol. 77, p. 105663, 2021.

[27] Ş. Koçyiğit, M.E. Emiroğlu, "The effect of the throat length and the hole diameter in throat portion of the venturi nozzle on aeration efficiency," *International Journal of Pure and Applied Sciences*, vol. 10, no. 1, pp. 125-135, 2024.

[28] J.X. Zhang, "Analysis on the effect of venturi tube structural parameters on fluid flow," *AIP Advances*, vol. 7, no. 6, p. 065315, 2017.

[29] Y. Zhou, J. Cui, Z. Chen, J. Liu, L. He, W. Fan, et al., "Parametric analysis of venturi-type microbubble generator and the bubble fragmentation dynamics," *Desalination and Water Treatment*, vol. 322, p. 101116, 2025.

[30] Q. Li, X. Guo, D. Z. Ming, M. Lei, J. L. Liu, L. Fang, et al., "Mechanism of microbubbles and cavitation effect on bubble breakage in a venturi bubble generator," *Journal of Applied Fluid Mechanics*, vol. 16, no. 4, pp. 778-793, 2023.

[31] X. Wang, Y. Shuai, H. Zhang, J. Sun, Y. Yang, Z. Huang, et al., "Bubble breakup in a swirl-venturi microbubble generator," *Chemical Engineering Journal*, vol. 403, p. 126397, 2020.

[32] Y. Liu, B. Li, "Numerical investigation of the cavitation characteristics in venturi tubes: The role of converging and diverging sections," *Applied Sciences*, vol. vol. 13, no. 13, p. 7476, 2023.

[33] L. Zhao, Z. Mo, L. Sun, G. Xie, H. Liu, M. Du, et al., "A visualized study of the motion of individual bubbles in a venturi-type bubble generator," *Progress in Nuclear Energy*, vol. 97, p. 74-89, 2017.

[34] H.S. Alam, M.I. Arif, T.A.F. Soelaiman, P. Sutikno, A.T. Sugiarto, A. Yusuf, "Experimental and numerical study of bubbly flow and bubble size distribution produced by swirling flow bubble generator," *Results in Engineering*, vol. 27, p. 106099 2025.

[35] J. RuanJ. Ruan, H. Zhou, Z. Ding, Y. Zhang, L. Zhao, J. Zhang, et al., "Machine learning-aided characterization of microbubbles for venturi bubble generator," *Chemical Engineering Journal* vol. 465, p. 142763, 2023.

[36] A. Fujiwara, K. Okamoto, K. Hashiguchi, J. Peixinho, S. Takagi, Y. Matsumoto, "Bubble breakup phenomena in a venturi tube," in *Proceedings of FEDSM2007*, vol. 42886, pp. 553-560, 2007.

[37] N. Niellambare, H.H. Mohamad, A.A. Erny, H.J. Nasrul, "Investigation on the effect of venturi geometry variation on microbubble generation," *AIP Conference Proceedings*, vol. 2610, no. 1, p. 050009, 2022.